JOURNAL OF MAGNETIC RESONANCE **135,** 260–264 (1998)
ARTICLE NO. MN981542

Resolution Improvements in *in Vivo* ^{1}H NMR Spectra with Increased Magnetic Field Strength

Rolf Gruetter,* Sally A. Weisdorf,† Vasantham Rajanayagan,* Melissa Terpstra,* Hellmut Merkle,* Charles L. Truwit,* Michael Garwood,* Scott L. Nyberg,‡ and Kâmil Uğurbil*

**Department of Radiology and †Department of Pediatrics, University of Minnesota, Minneapolis, Minnesota 55112; and ‡Department of Surgery, Mayo Clinic, Rochester, Minnesota*

E-mail: gruetter@geronimo.drad.umn.edu

Received March 18, 1998

The measurement of cerebral metabolites using highly homologous localization techniques and similar shimming methods was performed in the human brain at 1.5 and 4 T as well as in the dog and rat brain at 9.4 T. In rat brain, improved resolution was achieved by shimming all first- and second-order shim coils using a fully adiabatic FASTMAP sequence. The spectra showed a clear improvement in spectral resolution for all metabolite resonances with increased field strength. Changes in cerebral glutamine content were clearly observed at 4 T compared to 1.5 T in patients with hepatic encephalopathy. At 9.4 T, glutamine H4 at 2.46 ppm was fully resolved from glutamate H4 at 2.37 ppm, as was the potential resonance from γ-amino-butyric acid at 2.30 ppm and N-acetyl-aspartyl-glutamate at 2.05 ppm. Singlet linewidths were found to be as low as 6 Hz (0.015 ppm) at 9.4 T, indicating a substantial decrease in ppm linewidth with field strength. Furthermore, the methylene peak of creatine was partially resolved from phosphocreatine, indicating a close to 1:1 relationship in gray matter. We conclude that increasing the magnetic field strength increases spectral resolution also for ^{1}H NMR, which can lead to more than linear sensitivity gains.

Key Words: **brain**; **magnetic field**; *in vivo*; **^{1}H NMR**; **resolution.**

INTRODUCTION

High-resolution NMR spectroscopy of solution samples benefits from increasing the field strength due to increases in sensitivity and spectral resolution. *In vivo,* the improvements in spectral resolution are more difficult to achieve due to sample and tissue dependent susceptibility effects. The latter can be regarded as microscopic susceptibility effects caused by paramagnetic species, which may be present in, e.g., microvessels. Linebroadening due to such microscopic susceptibility effects is extremely difficult to eliminate *in vivo.* When studying excised tissue, a recent study has shown that dramatic improvements in spectral resolution are possible when using magic-angle spinning (*1*). Macroscopic susceptibility effects are caused mainly by the air–tissue or bone–tissue interface and depend on geometry and orientation. As such the macroscopic field variations in space can be reduced by adjusting shim coil correction currents. Many shim methods have been described (*2–10*). Most have used linear shim coils (*X, Y, Z*) while some have extended their shim procedures to higher order, including the adjustment of second-order shimming using FASTMAP in the past several years (*11–13*).

Tissue-induced susceptibility effects appear to be less detrimental for *in vivo* ^{31}P NMR where the improvements in resolution with high-field were demonstrated early by several groups, e.g., (*14, 15*), and are now well accepted. Likewise, spectral improvements with field strength have been quite dramatic for ^{13}C as evidenced by a comparison of spectra of the human brain acquired at 1.5 T (*16*) to those acquired at 2.1 T (*17–19*) and to those achieved at 4 T (*20*). Some of these improvements can be attributed to using second-order shimming, such as FASTMAP (*12*). For ^{1}H spectroscopy, improvements with high magnetic fields have been less obvious, although it has been noted that spectral resolution in small-voxel CSI data sets is clearly improved at 4 T (*21*). Improvements with ^{1}H spectroscopy are harder to realize since the proton spectrum depends much more on very high spectral resolution due to the more crowded spectrum and higher gyromagnetic ratio.

Expectations that spectral resolution indeed increases with magnetic fields were recently confirmed by the demonstration that the glucose peak at 5.23 ppm was readily observable in human brain at 4 T (*22*). We therefore sought to extend these comparisons to the entire proton spectrum and specifically compare them to spectra obtained at 1.5 T. In order to estimate what spectral improvements can be expected when studying humans at field strengths significantly above 4 T, we also measured dog and rat brain spectra at 9.4 T.

RESULTS AND DISCUSSION

To maximize spectral resolution *in vivo,* the susceptibility effects due to tissue boundaries must be reduced, or, if possible, eliminated. At 1.5 T, it may be sufficient to use the linear shim coils for many applications; however, since susceptibility

1090-7807/98 $25.00

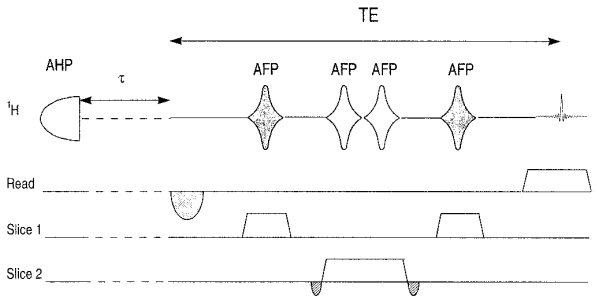

FIG. 1. Fully adiabatic FASTMAP pulse sequence used for shimming surface coil NMR of rat brain at 9.4 T. Pairs of adiabatic full passage (AFP) pulses (hyperbolic secant) are used to rephase coherences in the corresponding slice 1 and slice 2. A 3-ms adiabatic half passage (AHP) pulse is used to convert the *z*-magnetization to transverse magnetization. The delay τ is applied on alternate scans to encode the B_o field as a phase shift. Refocusing gradient lobes are indicated by the hashed areas.

effects increase linearly with static field, higher-order terms become increasingly important. Shimming of *in vivo* human tissue requires extremely efficient methods that minimize the time needed for this critical adjustment (*2, 5, 6, 8, 12, 23*). One of these techniques, *f*ast, *a*utomatic, *s*himming *t*echnique by *m*apping *a*long *p*rojections, FASTMAP, has proven to be useful for human applications at high fields. FASTMAP was originally based on stimulated echo generation (*11–13*), albeit it was recognized that adiabatic refocusing pulses can improve sensitivity and thus reliability dramatically, as judged from the noise error propagation provided. Such an improvement of FASTMAP was described recently, resulting in a semi-adiabatic pulse sequence leading to at least a two-fold improvement of the signal and improvements in reliability (*24*). At 4 T we found the use of the stimulated echo sequence to be satisfactory. For *in vivo* shimming of the rat brain, we used a fully adiabatic FASTMAP sequence (Fig. 1) that uses adiabatic excitation combined with two adiabatic slice selection pulses consisting of pairs of hyperbolic secant pulses to rewind the incurred phase distortions across the slice produced by each adiabatic full-passage pulse (*25*). The first slice selection pulse was generated by two adjacent adiabatic inversion pulses, whereas the other slice selection process was placed symmetrically about these pulses, as in a previously described method (*26*). As in previous implementations of FASTMAP (*11–13, 24*), the B_o field was encoded by measuring the phase difference of the resulting projections measured from the displacement of the Hahn spin-echo from the gradient echo by the delay τ placed after the 90° excitation pulse. Shimming using the FASTMAP sequence of Fig. 1 was extremely reliable in the rat brain resulting in water linewidths of 11.5–15 Hz for 64 μl voxels.

Comparison of spectra obtained in the human brain at 1.5 T (Fig. 2A) and 4 T (Fig. 2B) was performed for a healthy subject and a patient with hepatic encephalopathy. The spectra were processed identically using 1 Hz exponential linebroadening. Signal changes due to elevated cerebral glutamine were readily observed at 4 T at 2.46 ppm (Fig. 2B) as was the decrease in *myo*-inositol reported previously, see (*27*) and references therein. The FASTMAP shim method used at 4 T led to highly reproducible linewidths and shapes that allowed subtraction of individual spectra from different subjects. To illustrate the reproducibility, a set of subtracted spectra is shown in Fig. 2C for two patients with hepatic encephalopathy. These spectra indicated that glutamine is the major signal change in these patients compared to normal adults. Previous difficulty in

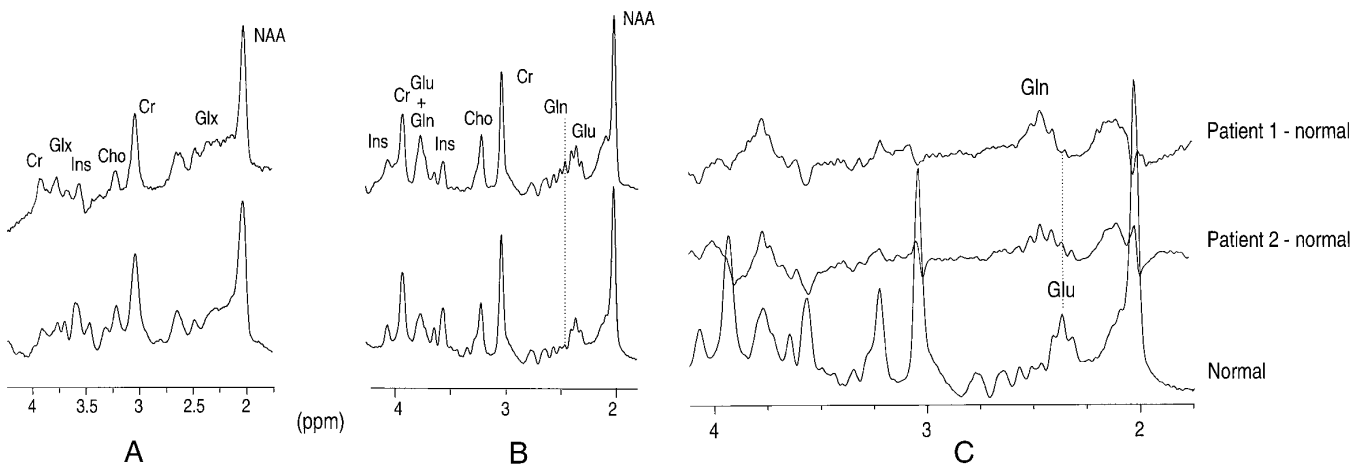

FIG. 2. ^{1}H NMR spectra acquired from the human brain at 1.5 T (A) and at 4 T (B) using STEAM (*TE* = 20ms, *TM* = 33 and 35 ms, respectively, *TR* = 3s). The bottom trace shows spectra acquired from a normal adult and the top spectra are from an 8-year-old patient with end-stage liver disease. Spectra were acquired on the same day at both fields from a 27-ml volume encompassing the visual cortex. (A) 1-Hz linebroadening was applied prior to FFT. In (C), difference spectra generated by subtracting the patient spectrum acquired from a normal adult are shown. The well defined and behaved baseline of the difference spectra illustrate the excellent, reproducible quality and lineshape achieved using FASTMAP at 4 T and that Gln dominates signal changes in hepatic encephalopathy. A tentative increase in choline signal at 3.22 ppm is also noted. When taking into account overlap with the H2 of *decreased myo*-Ins the true choline increase may actually have been underestimated, which further illustrates the need for spectral deconvolution approaches.

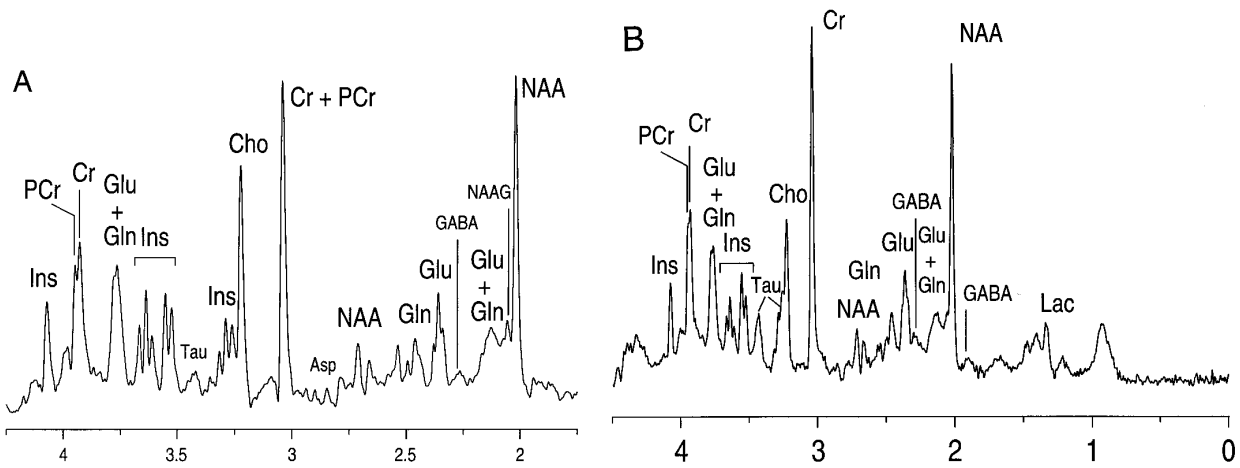

FIG. 3. (A) ^{1}H NMR spectrum acquired from a 1-ml volume lateral to the ventricle in dog brain at 9.4 T. Processing consisted of zero-filling, 3-Hz Lorentz-to-Gauss lineshape conversion and FFT. Peaks were tentatively assigned based on dominant constituent and published chemical shifts *28*). (B) This shows a spectrum acquired from a 64-μl volume in the rat sensorimotor cortex caudal to the striatum. Processing consisted of zero-filling, 3-Hz Lorentz-to-Gauss lineshape conversion and FFT.

quantifying specific glutamine changes at 1.5 T may be attributed to the similarity of the spectrum of glutamine to that of the glutamate spin system at lower field strengths, e.g., (*21*). We have extended the FASTMAP method to the 9.4-T 31-cm system to study the dog brain. In these spectra, water linewidths were between 12 and 18 Hz and NAA linewidths were between 6 and 12 Hz. Such a spectrum is shown in Fig. 3A and is representative of the spectral resolution that is reproducibly achievable. The spectra shown in Fig. 3 were processed with a modest resolution enhancement, i.e., a 3 Hz Lorentz-to-Gauss linewidth conversion. Several new features became apparent: (i) The partially resolved and clearly indicated homonuclear coupling (J = 6–7.5 *Hz*) corresponding to a triplet at 3.43 ppm and in the glutamate H4 peak at 2.37 ppm. The triplet-like structure at 3.43 ppm is consistent with this peak being mainly from taurine in dog brain. (ii) Spectral resolution led to the resolution of multiplet lines in *myo*-inositol (J = 9.5 *Hz*), clearly observed for the H2,4 and H4,6 peaks at 3.5–3.7 ppm and for the H5 peak at 3.28 ppm. (iii) Most importantly, the creatine (Cr) methylene peak is showing separation into two peaks, one at 3.95 and one at 3.93 ppm, corresponding to phosphocreatine (PCr) and the unphosphorylated form of Cr (*28*). This peak pattern was consistently observed in the dog brain spectra despite a high variability of voxel position. Separation of Cr and PCr was also inferred from the much broader linewidth of the creatine methylene resonance measured at 3.94 ppm in an infant at 4 T, consistent with the chemical shift of Cr and PCr, where the singlet linewidth was 3 Hz (not shown). (iv) The resolution of singlet lines was also clearly improved at 9.4 T, which was apparent by the reliable and consistent observation of a small resonance at 2.05 ppm, previously assigned to the neurotransmitter N-acetyl-aspartyl-glutamate, NAAG (*29–31*). (v) The resolution of coupled peaks, such as the CH_2 from glutamate and glutamine, and GABA indicates that these peaks are now clearly resolved, suggesting the potential of measuring GABA at 2.30 ppm without the need of spectral *J*-editing in animal brain at such high fields.

The results shown herein for dog brain were consistent with those achieved in rat brain, where the water linewidth was between 11.5 and 16 Hz throughout and the NAA linewidths ranged between 6 and 11 Hz. Such a spectrum is shown in Fig. 3B, which also indicates improved resolution of lactate at 1.33 ppm from the broad background resonances, which have been attributed to macromolecules (*32*).

The stack plot in Fig. 4 shows spectra acquired at 1.5, 4, and 9.4 T to illustrate improvements in spectral resolution with higher magnetic field strength. Note in particular that the linewidths of the prominent singlets NAA, Cr, and Cho decrease with field strength. Improved spectral resolution is expected to translate into a much improved sensitivity for those resonances that are difficult to resolve at lower magnetic fields, and thus may substantially amplify sensitivity improvements beyond the linear increase predicted from theory. Improved resolution can be expected for spin systems such as glucose, taurine, glutamine, N-acetyl-aspartate, aspartate, PCr, and Cr; peak fitting methods such as LCModel (*33*) are expected to perform substantially better for these and other peaks such as *myo*-inositol, *scyllo*-inositol, glutamate, and lactate.

The water linewidth decreased from approximately 0.04 ppm in the human brain at 4 T to approximately 0.02 ppm in the dog and rat brain at 9.4 T. Such decreases in linewidth may be exploited to achieve an improved baseline stability around water, essential for the detection of resonances such as the 5.23 ppm peak of glucose (*22*) and the methine proton of lactate, which was reliably observed at 9.4 T in postmortem spectra of brain and muscle (not shown). ^{1}H NMR spectra acquired from human muscle at 4 T and rat muscle at 9.4 T showed improvements in resolution similar to those spectra acquired from brain.

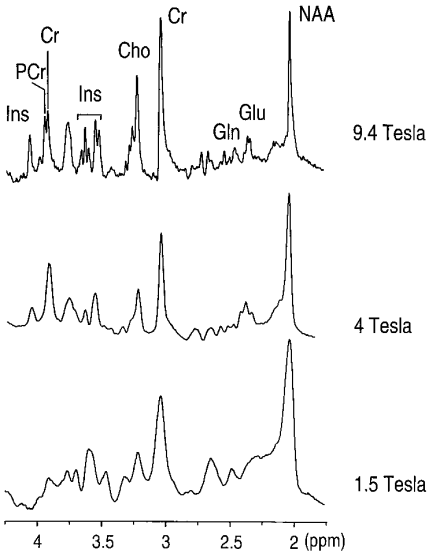

FIG. 4. Comparison of increases in spectral resolution with magnetic field strength. The stack plot shows corresponding spectra from 27-ml volumes in the human occipital lobe at 1.5 T (bottom) and at 4 T (middle) and a 1-ml spectrum from dog brain acquired at 9.4 T (top). Note the apparent decrease in singlett linewidths at the NAA, Cr, and Cho positions, which is direct and unequivocal evidence for increased spectral resolution *in vivo.*

Recently, a strong signal has been reported at 2.4 ppm in ^{1}H spectra acquired at 0.5 T (*34*), which can be explained by multiplet collapse of the glutamate and glutamine H4 and H3 resonances leading to an apparent singlet resonance with an intensity equivalent to that from 4 protons. Assuming a concentration of 10–12 m*M* for the sum of glutamate, glutamine, and GABA, the corresponding peak area would indeed be comparable to that observed for NAA, but critical information on the individual components is lost.

The spectra obtained at 9.4 T showed a distinct species-specific difference between the rat and dog brain at the taurine chemical shift (3.43 ppm). In the rat brain spectrum, a prominent Tau peak was observed, the area of which was larger than the *myo*-inositol (Ins) triplet at 4.07 ppm (Fig. 3B) which suggests that the major constituent of the choline resonance may be from taurine and inositol in short *TE* spectra, which was consistent with the multiplet pattern observed due to the lower *J* of taurine (approximately 6 Hz) as opposed to 9 Hz for Ins and previous assignments in rat brain (*35*). In the dog brain, however, the Tau triplet at 3.43 ppm is smaller (Fig. 3A), and the multiplet structure (apparent $J \sim$ 9 Hz) at 3.28 ppm is dominated by Ins.

CONCLUSION

The improvements demonstrated for ^{1}H NMR of brain are expected to translate into significant improvements in sensitivity for many more metabolites. The results suggest that in addition to choline, (phospho)creatine, NAA, and lactate, a comprehensive neurochemical profile can be measured non-invasively, which is expected to amplify the diagnostic power and neurochemical value of ^{1}H NMR well beyond currently available capabilities.

EXPERIMENTAL

Human subjects were studied at 1.5 and 4 T after giving informed consent according to procedures and forms approved by the Institutional Review Board.

Localization of volumes of interest was based on anatomic images using T_1-weighted imaging. To facilitate direct comparison, volumes were placed in the occipital cortex to encompass the primary visual cortex. Volume size was a cube with 3-cm sides (27mL). Shimming was performed using manufacturer-supplied MAPshim at 1.5 T and FASTMAP at 4 T (*22*). At 1.5 T, we used the manufacturer-supplied STEAM sequence with $TR = 3$ s, $TE = 20$ ms, and $TM = 35$ ms. After shimming the whole head water signal using manufacturer-supplied MAPshim, the occipital volume was handshimmed at 1.5 T using the linear shim coils and the Z2 shim coil. At 4 T, single-voxel localization was based on STEAM (*36*) implemented as 3,1-DRYSTEAM (*37*) as described previously (*33*). Repetition time *TR* was 3 s, echo time *TE* was 20 ms, and *TM* was 33 ms.

At 9.4 T, we used localization sequences identical to those used at 4 T, except TM was slightly increased to 36 ms. The shim procedure was an implementation of FASTMAP identical to that at 4 T (*13*), except that for shimming the *rat* brain we used the fully adiabatic FASTMAP pulse sequence shown in Fig. 1. As in the original implementation of FASTMAP (*12*), the sequence relies on measuring the phase difference of projections acquired with an extra delay τ in the first echo period to those acquired without such a delay, which encodes B_o inhomogeneity without any confounding effects from eddy currents, which were minimized on both high-field systems using methods and procedures described elsewhere (*38*). Excitation was performed using a numerically optimized adiabatic half passage pulse (*39*). Refocusing of the magnetization was achieved with adiabatic 180° pulses, consisting of two hyperbolic secant pulses for each slice selection (3300-Hz bandwidth). Such use of the hyperbolic secant pulses ensured that phase modulation across the slice was eliminated, leading to full adiabaticity and thus maximized sensitivity (*25, 26*). The sequence was verified to perform adiabatically in phantom experiments by measuring the projection signal along the surface coil axis while increasing pulse power. Adiabatic performance was confirmed by observing that the projection signal was independent of RF pulse power above a certain threshold.

ACKNOWLEDGMENTS

Supported by NIH Grants RR08079 and CA64338, the W.M. Keck Foundation, and the Mayo Medical Foundation.

REFERENCES

1. L. L. Cheng, M. J. Ma, L. Becerra, T. Ptak, I. Tracey, A. Lackner, and R. G. Gonzalez, Quantitative neuropathology by high resolution

magic angle spinning proton magnetic resonance spectroscopy, *Proc. Natl. Acad. Sci. USA* **94,** 6408–6413 (1997).

2. T. G. Reese, T. L. Davis, and R. M. Weisskoff, Automated shimming at 1.5 T using echo-planar image frequency maps, *J. Magn. Reson. Imaging* **5,** 739–745 (1995).
3. J. Hu, T. Javaid, F. Ariasmendoza, Z. Liu, R. Mcnamara, and T. R. Brown, A fast, reliable, automatic shimming procedure using H-1 chemical-shift-imaging spectroscopy, *J. Magn. Reson. B* **108,** 213–219 (1995).
4. P. C. M. van Zijl, S. Sukumar, M. O. Johnson, P. Webb, and R. E. Hurd, Optimized shimming for high-resolution NMR using three-dimensional image-based field mapping, *J. Magn. Reson. A* **111,** 203–207 (1994).
5. E. Schneider and G. Glover, Rapid in vivo proton shimming, *Magn. Reson. Med.* **18,** 335–347 (1991).
6. S. Kanayama, S. Kuhara, and K. Satoh, In vivo rapid magnetic field measurement and shimming using single scan differential phase mapping, *Magn. Reson. Med.* **36,** 637–642 (1996).
7. F. A. Jaffer, H. Wen, R. S. Balaban, and S. D. Wolff, A method to improve the B-O homogeneity of the heart in vivo, *Magn. Reson. Med.* **36,** 375–383 (1996).
8. P. Webb and A. Macovski, Rapid, fully automatic, arbitrary-volume in vivo shimming, *Magn. Reson. Med.* **20,** 113–122 (1991).
9. M. G. Prammer, J. C. Hazelgrove, M. Shinnar, and J. S. Leigh, *J. Magn. Reson.* **77,** (1988).
10. J. Tropp, K. A. Derby, C. Hawrysko, S. Sugiura, and H. Yamagata, *J. Magn. Reson.* **85,** 244 (1989).
11. R. Gruetter and C. Boesch, Fast, Non-iterative shimming on spatially localized signals: In vivo analysis of the magnetic field along axes, *J. Magn. Reson.* **96,** 323–334 (1992).
12. R. Gruetter, Automatic, localized in vivo adjustment of all first- and second-order shim coils, *Magn. Reson. Med* **29,** 804–811 (1993).
13. R. Gruetter and K. Ugurbil, A fast, automatic shimming technique by mapping along projections (FASTMAP) at 4 Tesla, *In "3rd Annual Meeting ISMRM,* Nice, 1995," p. 698.
14. M. D. Boska, B. Hubesch, D. J. Meyerhoff, D. B. Twieg, G. S. Karczmar, G. B. Matson, and M. W. Weiner, Comparison of 31P MRS and 1H MRI at 1.5 and 2.0 T, *Magn. Reson. Med* **13,** 228–238 (1990).
15. S. Weisdorf, K. Hendrich, H. Merkle, K. Ugurbil, and M. Garwood, Improvement in signal to noise ratio and resolution for in vivo localized 31P spectroscopy with increasing field strengths at 2, 4.7, and 7 Tesla, *In "Soc. Magn. Reson. Med.,* San Francisco, 1991," p. 491.
16. N. Beckman, J. Seelig, and H. Wick, Analysis of glycogen storage disease by in vivo 13C NMR: Comparison of normal volunteers with a patient, *Magn. Reson. Med.* **16,** 150 (1990).
17. R. Gruetter, D. L. Rothman, E. J. Novotny, and R. G. Shulman, Localized 13C NMR spectroscopy of myo-inositol in the human brain in vivo, *Magn. Reson. Med.* **25,** 204–210 (1992).
18. R. Gruetter, E. J. Novotny, S. D. Boulware, D. L. Rothman, G. F. Mason, G. I. Shulman, R. G. Shulman, and W. V. Tamborlane, Direct measurement of brain glucose concentrations in humans by 13C NMR spectroscopy, *Proc. Natl. Acad. Sci. USA* **89,** 1109–1112 (1992).
19. R. Gruetter, E. J. Novotny, S. D. Boulware, G. F. Mason, D. L. Rothman, J. W. Prichard, and R. G. Shulman, Localized 13C NMR spectroscopy of amino acid labeling from [1-13C] D-glucose in the human brain, *J. Neurochem.* **63,** 1377–1385 (1994).
20. R. Gruetter, G. Adriany, H. Merkle, and P. M. Andersen, Broadband decoupled, 1H localized 13C MRS of the human brain at 4 Tesla, *Magn. Reson. Med.* **36,** 659–664 (1996).
21. G. F. Mason, J. W. Pan, S. L. Ponder, D. B. Twieg, G. M. Pohost, and H. P. Hetherington, Detection of brain glutamate and glutamine in spectroscopic images at 4.1T, *Magn. Reson. Med.* **32,** 142–145 (1994).
22. R. Gruetter, M. Garwood, K. Ugurbil, and E. R. Seaquist, Observation of resolved glucose signals in 1H NMR spectra of the human brain at 4 Tesla, *Magn. Reson. Med.* **36,** 1–6 (1996).
23. A. M. Blamire, D. L. Rothman, and T. Nixon, Dynamic shim updating—A new approach towards optimized whole brain shimming, *Magn. Reson. Med.* **36,** 159–165 (1996).
24. J. Shen, R. E. Rycyna, and D. L. Rothman, Improvements on an in vivo automatic shimming method (FASTERMAP), *Magn. Reson. Med.* **38,** 834–839 (1997).
25. S. Conolly, G. Glover, D. Nishimura, and A. Macovski, A reduced power selective adiabatic spin-echo pulse sequence, *Magn. Reson. Med.* **18,** 28–38 (1991).
26. R. A. de Graaf, Y. Luo, M. Garwood, and K. Nicolay, B_1-insensitive, single-shot localization and water suppression, *J. Magn. Reson. B* **113,** 35–45 (1996).
27. B. D. Ross, E. R. Danielsen, and S. Bluml, Proton magnetic resonance spectroscopy: The new gold standard for diagnosis of clinical and subclinical hepatic encephalopathy? *Dig. Dis.* **14,** 30–39 (1996).
28. W. Willker, J. Engelmann, A. Brand, and D. Leibfritz, Metabolite identification in cell extracts and culture media by proton-detected 2D-H,C-NMR spectroscopy, *J. MR Anal.* **2,** 21–32 (1996).
29. P. J. Pouwels and J. Frahm, Differential distribution of NAA and NAAG in human brain as determined by quantitative localized proton MRS, *NMR Biomed.* **10,** 73–78 (1997).
30. D. Holowenko, J. Peeling, and G. Sutherland, 1H NMR properties of N-acetylaspartylglutamate in extracts of nervous tissue of the rat, *NMR Biomed.* **5,** 43–47 (1992).
31. P. B. Barker, S. N. Breiter, B. J. Soher, J. C. Chatham, J. R. Forder, M. A. Samphilipo, C. A. Magee, and J. H. Anderson, Quantitative proton spectroscopy of canine brain: In vivo and in vitro correlations, *Magn. Reson. Med.* **32,** 157–163 (1994).
32. K. L. Behar, D. L. Rothman, D. D. Spencer, and O. A. C. Petroff, Analysis of macromolecule resonances in 1H MR spectra of human brain, *Magn. Reson. Med.* **32,** 294–302 (1994).
33. S. W. Provencher, Estimation of metabolite concentrations from localized in vivo proton NMR spectra, *Magn. Reson. Med.* **30,** 672–679 (1993).
34. R. W. Prost, L. Mark, M. Mewissen, and S. J. Li, Detection of glutamate/glutamine resonances by 1H magnetic resonance spectroscopy at 0.5 tesla, *Magn. Reson. Med.* **37,** 615–618 (1997).
35. W. Dreher and D. Leibfritz, On the use of two-dimensional-J NMR measurements for in vivo proton MRS: Measurement of homonuclear decoupled spectra without the need for short echo times, *Magn. Reson. Med.* **34,** 331–337 (1995).
36. D. Matthaei, J. Frahm, A. Haase, K. D. Merboldt, and W. Hanicke, Multipurpose NMR imaging using stimulated echoes, *Magn. Reson. Med.* **3,** 554–561 (1986).
37. C. T. W. Moonen and P. C. M. van Zijl, Highly effective water suppression for in vivo proton NMR spectroscopy (DRYSTEAM), *J. Magn. Reson.* **88,** 28–41 (1990).
38. M. Terpstra, P. Andersen, and R. Gruetter, Localized eddy current compensation using quantitative field mapping, *J. Magn. Reson.* **131,** 139–143 (1998).
39. K. Ugurbil, M. Garwood, and A. Rath, Optimization of modulation functions to improve insensitivity of adiabatic pulses to variations in B_1 magnitude, *J. Magn. Reson.* **80,** 448–469 (1988).